

Heavy metal complexes of 4-chlorodipicolinic acid - structural, spectral and thermal correlations

Z. Vargová, M. Almáši, R. Gyepes & R. Vetráková

To cite this article: Z. Vargová, M. Almáši, R. Gyepes & R. Vetráková (2019): Heavy metal complexes of 4-chlorodipicolinic acid - structural, spectral and thermal correlations, Journal of Coordination Chemistry, DOI: [10.1080/00958972.2019.1675873](https://doi.org/10.1080/00958972.2019.1675873)

To link to this article: <https://doi.org/10.1080/00958972.2019.1675873>

 View supplementary material 

 Published online: 12 Oct 2019.

 Submit your article to this journal 

 View related articles 

 View Crossmark data 



Heavy metal complexes of 4-chlorodipicolinic acid - structural, spectral and thermal correlations

Z. Vargová^a, M. Almáši^a, R. Gyepes^b and R. Vetráková^a

^aDepartment of Inorganic Chemistry, Faculty of Science, P. J. Šafárik University, Košice, Slovak Republic; ^bDepartment of Inorganic Chemistry, Faculty of Science, Charles University, Praha, Czech Republic

ABSTRACT

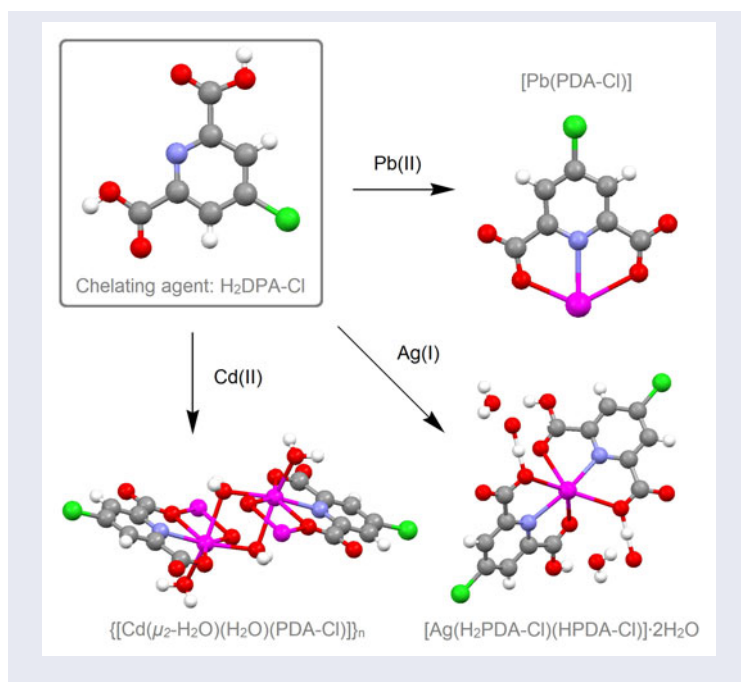
The ligand, 4-chloro-2,6-dipicolinic acid (H₂PDA-Cl), and its two heavy metal complexes, [Ag(HDPA-Cl)(H₂DPA-Cl)·2H₂O] (**1**) and {[Cd(μ₂-H₂O)(H₂O)(PDA-Cl)]_n} (**2**), were prepared and then characterized by single-crystal X-ray diffraction. In addition, spectral and thermal correlations with structural results complete their solid-state description and facilitate complex **3** ([Pb(DPA-Cl)]) composition determinations. Complex **1** crystallizes in a monoclinic space group *C2/c* and each DPA-Cl ligand is tridentate to Ag(I) through the pyridine N and two monodentate carboxyl O atoms. The carboxy group with carbonyl C1 is semideprotonated and forms a symmetric hydrogen bond with a carboxy group of a neighboring complex. Complex **2** crystallizes in a triclinic lattice with space group *P*. The Cd(II) ions are seven-coordinate and the coordination polyhedra can be described as a distorted pentagonal bipyramid. IR data are consistent with monodentate coordination of the carboxylate to Ag(I), Cd(II), and Pb(II) and observed wavenumber shifts confirm PDA-Cl ligand coordination to Pb(II) in **3**. Thermal stability of anhydrous complexes indicates the metal-ligand interactions. The thermal stability of prepared compounds is reflected by the strength of interaction between metal-ligand and hydrogen bonds.

ARTICLE HISTORY

Received 14 February 2019
Accepted 9 September 2019

KEYWORDS

Lead; cadmium; silver; chelating agent; coordination



1. Introduction

Environmental pollution by heavy metals is found increasingly in military, industrial and agricultural zones. Fuel and power industries generate 2.4 million tons of As, Cd, Cr, Cu, Hg, Ni, Pb, Se, V, and Zn. Metals, discharged or transported into the environment, may undergo transformations and can have large environmental, public health and economic impact [1]. Many different methods are available for removal of toxic metal ions. Among them, the most commonly used are ion exchange, adsorption, reduction, and precipitation. In many cases, the environmentally most compatible and cost-effective solutions include combination of two or more of these processes.

Chelating agents are offered as one solution and are widely used in many industrial, domestic and agriculture applications due to their ability to complex metals. They have been used in applications, such as scale and corrosion inhibitors, pulp, paper and textile production, cleaning and laundry operations, prevention/inhibition of the growth of microorganisms, soil remediation, waste and effluent treatment, agriculture, metal electroplating and other surface treatments, tanning processes, cement admixtures, photography, food products, pharmaceuticals, and cosmetics. Among the common chelating agents, organophosphonates and aminopolycarboxylates (APCs) stand out as they are good metal chelators with a good quality/price ratio [2].

The chelating agent pyridine-2,6-dicarboxylic acid (H_2PDA), also known as dipicolinic acid, contains a pyridine ring and carboxylic functions with N- and O-donors. Due to its structure, it tends to chelate metals in a proportion of 2:1 (ligand/metal), improving the stability of the complex [2]. Moreover, PDA is a low toxic and ready-biodegradable compound according to the OECD guidelines [3]. Due to its ability to complex with metal

ions, it has been studied for remediation of soils, used in detergents and cleaning applications.

To test the chelating ability of 4-chloro-2,6-dipicolinic acid (4-chloro-2,6-pyridinedicarboxylic acid, H₂PDA-Cl), we prepared the chlorine-functionalized variant that can be a prospective ligand in many areas from the structural points of view. Previous results revealed that chlorine function is not connected directly to metals and the N- and O-atoms remain as donors. However, this function contributes significantly to intermolecular interactions, frequently through hydrogen bonding with secondary entities such as solvent molecules [4–11].

In 1999, Shaw et al. demonstrated promising separations involving HPCIC (high performance chelation ion chromatography) using polystyrene-divinyl (PS-DVB) resin dynamically modified with H₂PDA-Cl. The retention order found for transition and heavy metal ions was U(VI) > Fe(III) > lanthanides > Cd(II) > Pb(II) > Cu(II) > Zn(II) > Ni(II) > Co(II) > Mn(II) using an eluent consisting of 1 M KNO₃ and 5 × 10⁻⁴ M H₂PDA-Cl at pH 1.2 (HNO₃). They concluded that PS-DVB dynamically modified with H₂PDA-Cl has promising results giving both, good peak efficiency and unusual metal selectivity [12].

Moreover, H₂PDA-Cl and other 4-substituted analogues, like chelators, were used for enhancement of terbium(III) and europium(III) complexes luminescence. Because of the ease which functional groups can be placed at the 4 position of dipicolinic acid, and the efficiency with which dipicolinic acid sensitizes lanthanide ion emission in aqueous solution, compounds of the type 4-X-dipicolinic acid represent attractive intermediates for formation of lanthanide energy transfer complexes with long emission lifetimes. In the case of Tb(III) complexes, maximum emission intensities were in the order: X = NH₂ > NHAc > OH > H > Cl > Br and measurements of emission decay kinetics revealed lifetimes of 1.0–2.0 ms [13]. However, the opposite trend was observed for Eu(III) complexes luminescence sensitization finding: X = Cl > H > OH [14] and the Eu(III) luminescence lifetime varied from 1.16 to 2.90 ms.

Further H₂PDA-Cl complexes testing was observed for insulin-enhancing activity in streptozotocin (STZ) induced diabetic Wistar rats. The effect of the chloro-substitution on lowering diabetic hyperglycaemia was evaluated and differences were found depending on the oxidation state [5]. There were observed significant differences in the abilities of H[V(PDA-Cl)₂].5.5H₂O.0.5NH₃ and [VO(PDA-Cl)(H₂O)₂] to lower diabetic hyperglycaemia when compared to the blood glucose levels in normal and diabetic rats. Moreover, in biological activity evaluation, a mixed-ligand Ni(II) complex ([Ni(PDA-Cl)(APYM)(H₂O)₂], APYM = 2-aminopyrimidine) was tested against three G⁺ and three G⁻ bacteria (the highest ATB activity was observed toward *S. epidermis*) and its fluorescence properties were studied in solvents with different dipole moments (fluorescence intensity increased in the order CH₃OH > H₂O > DMSO) [10].

To study toxic Cd(II), Pb(II), and Ag(I) metal ions–ligand H₂PDA-Cl interactions (and to compare H₂PDA-Cl coordination ability with H₂PDA) in aqueous solution and in solid state, we observed the fast crystals elimination from mother liquor at very low species concentrations. Therefore we decided to determine and characterize the metal complexes in the solid state and compare their structural, spectral, and thermal features. Unfortunately, all attempts to find solution experimental conditions failed

(metal/ligand concentrations, metal/ligand ratio). In all cases, at the beginning of the experiment, precipitates were produced.

2. Experimental

2.1. Materials and measurements

$\text{Cd}(\text{NO}_3)_2 \cdot 4\text{H}_2\text{O}$, $\text{Pb}(\text{NO}_3)_2$ and AgNO_3 were obtained from Lachema (Czech Republic). The ligand 4-chloropyridine-2,6-dicarboxylic acid was prepared by the reaction procedure described in Section 2.2.1. Chemicals used in the synthesis were obtained from Sigma-Aldrich or Acros Organics companies. All chemicals were analytically pure and used without purification. Demineralized water was used for all solution preparations.

2.2. Preparation of the complexes

2.2.1. Synthesis of 4-chloropyridine-2,6-dicarboxylic acid ($\text{H}_2\text{DPA-Cl}$)

4-Chloropyridine-2,6-dicarboxylic acid was prepared by two-step organic reactions from 4-hydroxypyridine-2,6-dicarboxylic acid (chelidamic acid) as a precursor and phenylphosphonic dichloride as a standard chlorinating agent. In the first step 2 g (10.92 mmol) of chelidamic acid and 10 cm³ (70.51 mmol) of phenylphosphonic dichloride were heated and stirred at 130 °C for 3 h in reflux under nitrogen. After selected reaction time, the mixture was cooled to laboratory temperature. During the reaction 4-chloropyridine-2,6-dicarbonyl dichloride was formed. To prepare the desired product, hydrolysis of acyl chloride was performed by addition of 50 cm³ water dropwise to the reaction mixture (be careful, strong exothermic reaction). The reaction residue was then suspended in distilled water, filtered off and slightly washed with ethanol, chloroform, diethyl ether and dried in a stream of air. Final product was isolated in the form of white powder with yield 1.43 g (65% based on chelidamic acid). Elem. analysis for $\text{C}_7\text{H}_4\text{Cl}_1\text{N}_1\text{O}_4$ (201.56 g.mol⁻¹) Calc. (Found) %: C, 41.71 (41.96); H, 2.00 (1.96); N, 6.95 (7.01). ¹H NMR (300 MHz, DMSO-*d*₆): $\delta = 8.24$ (s, 2 H) ppm; ¹³C NMR (100 MHz, DMSO-*d*₆): $\delta = 164.8, 150.1, 145.1, 127.2$. $\text{H}_2\text{DPA-Cl}$ in the form of single crystals suitable for single crystal X-ray analysis were prepared by recrystallization from mixture of solvents EtOH/H₂O (v:v, 2:1).

2.2.2. Synthesis of $[\text{Ag}(\text{H}_2\text{PDA-Cl})(\text{HPDA-Cl})] \cdot 2\text{H}_2\text{O}$ (1)

A solution of silver(I) nitrate (62.4 mg, 0.25 mmol) in ethanol/water (10 cm³, 2:1 molar ratio) was slowly added to a solution of $\text{H}_2\text{PDA-Cl}$ (50 mg, 0.25 mmol) in ethanol/water (40 cm³, 2:1 molar ratio). After 24 h the yellow precipitate of **1** was filtered and the clear solution was kept in the dark for evaporation. After a month, beige needles suitable for X-ray analysis were obtained. Elem. analysis for $\text{C}_{14}\text{H}_{11}\text{Ag}_1\text{Cl}_2\text{N}_2\text{O}_{10}$ (546.02 g.mol⁻¹) Calc. (Found) %: C, 30.79 (31.03); H, 2.03 (1.98); N, 5.13 (5.19), yield: 23 mg corresponding to 17%.

2.2.3. Synthesis of $\{[\text{Cd}(\mu_2\text{-H}_2\text{O})(\text{H}_2\text{O})(\text{PDA-Cl})]\}_n$ (2)

A solution of cadmium(II) nitrate tetrahydrate (95 mg, 0.25 mmol) in ethanol/water (10 cm³, 2:1 molar ratio) was slowly added to a solution of $\text{H}_2\text{PDA-Cl}$ (50 mg, 0.25 mmol) in ethanol/water (40 cm³, 2:1 molar ratio). After 24 h the yellow precipitate

of **2** was filtered and the clear solution was kept for slow evaporation. After a month, beige crystals suitable for X-ray analysis were afforded. Elem. analysis for $C_7H_6Cd_1Cl_1N_1O_6$ ($347.98 \text{ g mol}^{-1}$) Calc. (Found) %: C, 24.16 (24.05); H, 1.73 (1.70); N, 4.03 (3.92), yield: 31 mg corresponding to 36%.

2.2.4. Synthesis of [Pb(PDA-Cl)] (**3**)

A solution of lead(II) nitrate (66 mg, 0.20 mmol) in ethanol/water (30 cm^3 , 2:1 molar ratio) was slowly added to an aqueous solution of PDA-Cl (40 mg, 0.20 mmol, 40 cm^3). After 24 h the precipitate of **3** was filtered and the clear solution was kept for slow evaporation. The result of slow evaporation was polycrystalline material not suitable for single crystal X-ray analysis. Elem. analysis for $C_7H_2Pb_1Cl_1N_1O_4$ ($406.76 \text{ g mol}^{-1}$) Calc. (Found) %: C, 20.67 (20.53); H, 0.49 (0.25); N, 3.44 (3.34), yield: 46 mg corresponding to 57%.

2.3. Elemental analysis and infrared spectroscopy

The elemental analyses were performed on a CHNOS Elemental Analyzer Vario MICRO (Elemental Analyzer system GmbH). Infrared spectra were recorded on a Nicolet Avatar FT-IR 6700 spectrometer from 4000 to 400 cm^{-1} using KBr pellets. KBr pellets were prepared by grinding sample with potassium bromide in mass ratio 2:200.

2.4. NMR spectroscopy

^1H and ^{13}C NMR spectra were recorded with a Varian Mercury Plus 400 spectrometer at frequency of magnetic field 400 (^1H NMR) and 100 (^{13}C NMR) MHz, respectively, using TMS as the internal reference.

2.5. X-ray diffraction

Single-crystal diffraction data of the free ligand (CCDC number 1940563) and **1** (CCDC number 194056) and **2** (CCDC number 1940562) were collected on a Nonius Kappa four-circle CCD diffractometer equipped with an Apex II (Bruker) detector and a Cryostream Cooler (Oxford Cryosystems). In all cases, $\text{MoK}\alpha$ radiation was used ($\lambda = 0.71073 \text{ \AA}$) and reduction of collected data was carried out by diffractometer software. The phase problem was solved by intrinsic phasing and structure models were refined by full matrix least squares on F^2 using the Shelx program suite [15]. Non-hydrogen atoms were refined anisotropically. Hydrogens located on aromatic rings were included in their ideal positions with their isotropic thermal parameters fixed to $1.2 U_{eq}$. The figures of final crystal structures were drawn using DIAMOND [16] and Mercury [17] software. Detailed crystallographic data are given in Table 1.

2.6. Thermal analysis

Stability and thermal behavior of the prepared compounds were studied by thermogravimetry (TG) using TA instrument TGA Q-500 in air. Samples were heated in dynamic atmosphere of air (argon was used as a protecting gas) with air flow rate $60 \text{ cm}^3 \cdot \text{min}^{-1}$

Table 1. Crystal data and structure refinement summary for H₂DPA-Cl·H₂O, **1** and **2**.

| | H ₂ DPA-Cl·H ₂ O | 1 | 2 |
|--|---|--|---|
| Formula | C ₇ H ₆ Cl ₁ N ₁ O ₅ | Ag ₁ C ₁₄ H ₁₁ Cl ₁ N ₂ O ₁₀ | Cd ₁ C ₇ H ₆ Cl ₁ N ₁ O ₆ |
| Formula weight | 219.58 | 546.02 | 347.98 |
| Color | Colorless | Yellow | Yellow |
| Temperature (K) | 150(2) | 150(2) | 150(2) |
| Crystal system | Monoclinic | Monoclinic | Triclinic |
| Space group | <i>P</i> 2 ₁ | <i>C</i> 2/ <i>c</i> | <i>P</i> -1 |
| <i>a</i> (Å) | 5.1861(3) | 6.5673(3) | 5.3994(2) |
| <i>b</i> (Å) | 9.4760(6) | 11.6494(5) | 8.8389(4) |
| <i>c</i> (Å) | 8.5224(5) | 24.1220(12) | 10.5007(5) |
| α (°) | 90 | 90 | 101.207(2) |
| β (°) | 94.147(2) | 93.017(2) | 95.930(2) |
| γ (°) | 90 | 90 | 93.338(2) |
| λ (MoK α) (Å) | 0.71073 | 0.71073 | 0.71073 |
| <i>V</i> (Å ³) | 417.72(4) | 1842.90(15) | 487.38(4) |
| <i>Z</i> | 2 | 4 | 2 |
| <i>D</i> (calcd) (g.cm ⁻³) | 1.746 | 1.968 | 2.371 |
| μ (mm ⁻¹) | 0.452 | 1.443 | 2.527 |
| <i>F</i> [000] | 224 | 1080 | 336 |
| Crystal size (mm) | 0.299 × 0.240 × 0.142 | 0.451 × 0.298 × 0.276 | 0.584 × 0.278 × 0.114 |
| θ min, θ max (°) | 2.1114, 28.8561 | 1.691, 27.561 | 1.991, 27.499 |
| Reflections collected/unique | 5630/1924 | 8721/2138 | 9084/2199 |
| Data/restraints/parameters | 1924/1/136 | 2138/1/146 | 2199/4/151 |
| Goodness-of-fit on <i>F</i> ² | 1.056 | 1.251 | 1.054 |
| Final <i>R</i> indices [<i>I</i> > 2 σ (<i>I</i>)] | <i>R</i> ₁ = 0.0311, w <i>R</i> ₂ = 0.0739 | <i>R</i> ₁ = 0.0417, w <i>R</i> ₂ = 0.0902 | <i>R</i> ₁ = 0.0241, w <i>R</i> ₂ = 0.0605 |
| <i>R</i> indices (all data) | <i>R</i> ₁ = 0.0343, w <i>R</i> ₂ = 0.0754 | <i>R</i> ₁ = 0.0458, w <i>R</i> ₂ = 0.0918 | <i>R</i> ₁ = 0.0267, w <i>R</i> ₂ = 0.0622 |

and heating rate 10 °C·min⁻¹ from 25 to 800 °C. Before thermal measurements, gentle grinding of the samples and careful packing into the platinum crucibles were performed. The mass of samples used in the analyses was 10–15 mg. Thermoanalytical curves obtained were analyzed using the Origin 6.1 computational program [18].

3. Results and discussion

3.1. Single crystal X-ray studies

3.1.1. Crystal structure of H₂DPA-Cl·H₂O

The chloro derivative of dipicolinic acid was synthesized by the procedure described in Section 2.2.1. After slow evaporation of the solvents 4-chloropyridine-2,6-dicarboxylic acid crystallizes as a monohydrate, H₂DPA-Cl·H₂O (Figure 1a,b). Ligand preparation was confirmed by elemental analysis whose experimental and theoretical values are in agreement as well as by NMR spectroscopy. ¹H NMR spectra contain only one singlet at 8.24 ppm, corresponding to hydrogen in the *para* position and four signals in ¹³C NMR at 164.8, 150.1, 145.1, and 127.2 ppm for carbons. The crystal structure of prepared ligand has been re-determined by the single crystal X-ray diffraction with aim to use its structural data for **3** composition determination (using IR spectroscopy, Section 3.2). The compound crystallizes in a monoclinic space group *P*2₁, with cell dimensions *a* = 5.1861(3) Å, *b* = 9.4760(6) Å, *c* = 8.5224(5) Å, and β = 94.147(2)°. Racemic twinning was present and its batch scale factor was refined to 0.317. Nieger et al. [19] noted similar twinning. Detailed crystallographic data and refinement details for H₂DPA-Cl·H₂O are listed in Table 1 and Supplementary Information Table S1. Protonation does not occur on the

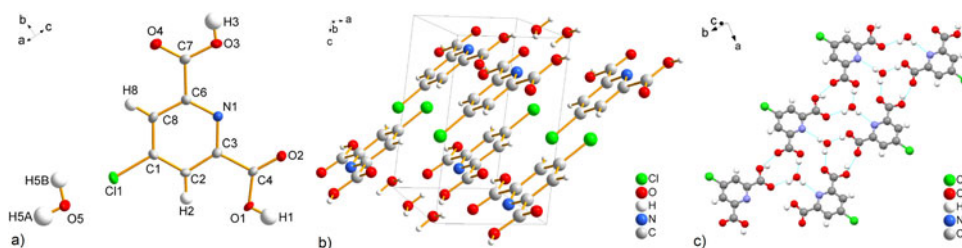


Figure 1. (a) A view of the crystal structure of 4-chloropyridine-2,6-dicarboxylic acid monohydrate. (b) Content of unit cell. (c) 1D supramolecular chains generated between H₂DPA-Cl and crystallization water molecules propagating along the *b* crystallographic axis.

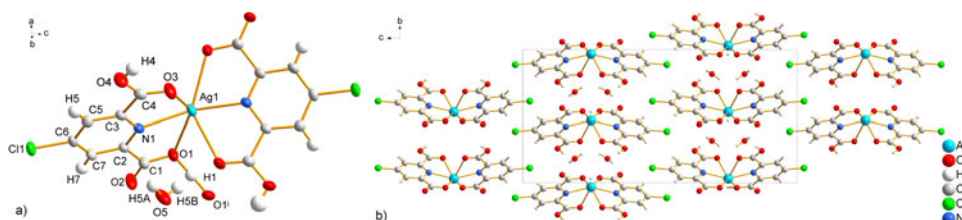


Figure 2. (a) The coordination environment of Ag(I) ion and coordination fashion of 4-chloropyridine-2,6-dicarboxylate ligand in the crystal structure of **1** ($i = -x + 2, y, -z + 1/2$). (b) Content of unit cell.

nitrogen of the pyridine ring and both carboxyl groups consist of carbonyl and hydroxyl groups. Each H₂DPA-Cl molecule generated O-H...O and O-H...N hydrogen bonds with crystallization water molecule to form endless chains propagated along the *b* crystallographic axis. Formation of 1D supramolecular polymeric chain is depicted in Figure 1c and hydrogen bond lengths and angles are summarized in Supplementary Information Table S2. Bond distances and angles are similar to the values presented previously [20] and they change in the range 1.374(4)–1.507(4) Å for C-C, 1.203(4)–1.217(4) Å for C-O, 117.0(3)–119.6(3)° for C-C-C and 110.8(3)°, 123.2(3)° for O-C-C.

3.1.2. Crystal structure of **1**

The crystal structure of [Ag(HDPA-Cl)(H₂DPA-Cl)·2H₂O] is depicted in Figure 2a,b and selected bond distances and angles are summarized in Supplementary Information Table S3. The prepared complex crystallized in a monoclinic lattice with space group *C2/c*, with cell dimensions $a = 6.5673(3)$ Å, $b = 11.6494(5)$ Å, $c = 24.1220(12)$ Å, $\beta = 93.017(2)^\circ$ and with four formula units in the unit cell. The asymmetric unit is formed of one silver(I), one ligand molecule and one crystal water molecule. Each DPA-Cl ligand is tridentate to Ag(I) through the pyridine N and two monodentate carboxyl O atoms. The silver is six-coordinate and the coordination polyhedron can be described as a distorted tetragonal bipyramid. The coordination environment is formed by four oxygens and two nitrogens of two crystallographically equivalent ligand molecules with a [AgN₂O₄] donor set. The interaction between Ag1-N1 (2.324(3) Å) is stronger than Ag1-O1 and Ag1-O3. The Ag1-O1/O3 distances are 2.558(3) Å and 2.617(6) Å, suggesting weak interactions. Although the Ag-O distances in **1** are longer,

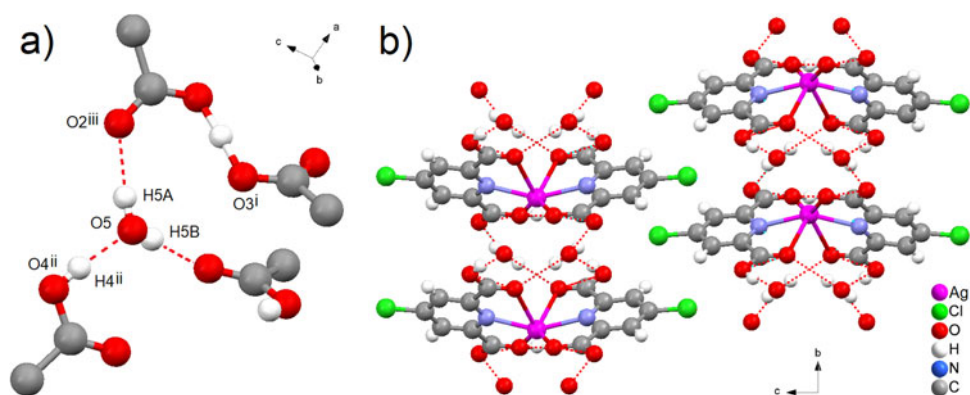


Figure 3. (a) Hydrogen bonds generated between carboxylic/carboxylate groups of ligand molecules and crystallization water molecule for **1** ($i = -x + 2, y, -z + 1/2$; $ii = x - 1, y, z$; $iii = x + 1/2, y + 1/2, z$). (b) Formation of final 2D supramolecular sheets.

they are comparable with bond distances of other silver complexes containing coordinated protonated carboxylic ligands [21–25].

The interesting feature of **1** is that carboxy group with carbonyl C1 is semideprotonated and forming a symmetric hydrogen bond with a carboxy group of a neighboring complex (Figure 3a). H1 lies on a center of symmetry and is involved in a strong O1-H1...O1ⁱ hydrogen bond ($i = -x + 2, y, -z + 1/2$; $d(D\cdots A) = 2.451(5)$ Å) and the O-H bond distance is 1.226(4) Å. Medium strength hydrogen bonds are formed between crystallization water molecules and carboxylic groups. O5 is an acceptor in O5...H4ⁱⁱ-O4ⁱⁱ ($ii = x - 1, y, z$; $d(D\cdots A) = 2.532(4)$ Å) hydrogen bond formation and donor for O2ⁱⁱⁱ ($iii = x + 1/2, y + 1/2, z$; $d(D\cdots A) = 2.686(4)$ Å) and O3ⁱ ($d(D\cdots A) = 2.933(4)$ Å). Hydrogen bonds are depicted in Figure 3a and corresponding bond lengths and angles are summarized in Supplementary Information Table S4.

The crystal structure shows **1** is a monomer, however, via formation of strong hydrogen bonds between adjacent complex units and medium strength hydrogen bonds formed through the crystallization water molecules, the final crystal packing of **1** is two-dimensional supramolecular sheets (Figure 3b).

For comparison, a similar complex, [Ag(HDPA)(H₂DPA)·2H₂O] [26, 27], was prepared using dipicolinate ligand (DPA). The coordination environment of Ag(I) ions and coordination fashion of DPA ligand is similar to **1**. The difference between our compound and [Ag(HDPA)(H₂DPA)·2H₂O] is in ligands and interactions of silver with donors. However, the bond distance between Ag-N in dipicolinate complex is similar (2.326(4) Å); the presence of chloro group as electron-withdrawing group on pyridine ring in DPA-Cl ligand had an impact on Ag-O bond lengths. Corresponding atom distances in **1** are longer (see text above) compared to [Ag(HDPA)(H₂DPA)·2H₂O] in which Ag-O bond lengths are 2.505(2) Å and 2.507(3) Å, indicating stronger interaction between coordinated carboxylic group and silver(I) ion.

3.1.3. Crystal structure of **2**

The cadmium(II) compound containing 4-chloropyridine-2,6-dicarboxylate was prepared as single crystals and the solid-state structure is depicted in Figure 4a–c. Results

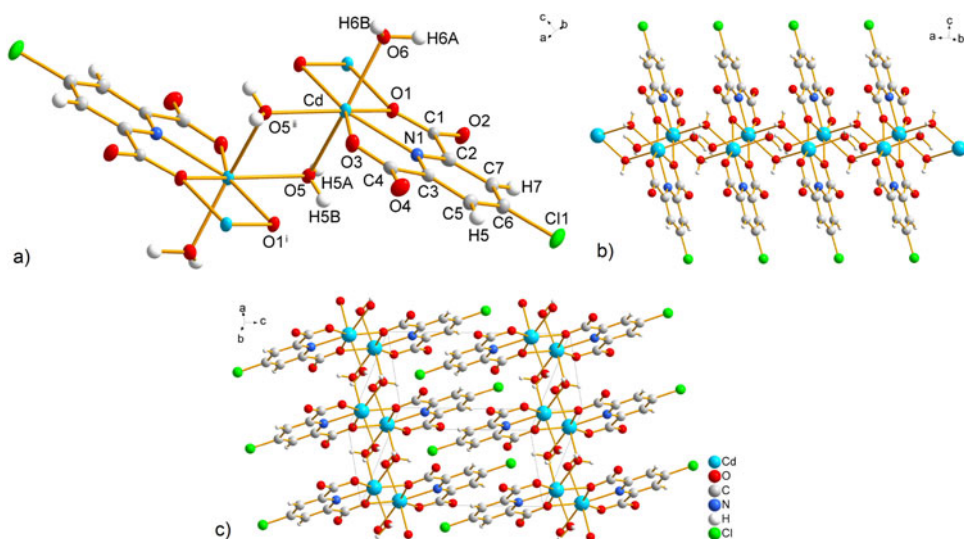


Figure 4. (a) Atomic labelling diagram of $\{[\text{Cd}(\mu_2\text{-H}_2\text{O})(\text{H}_2\text{O})(\text{PDA-Cl})]\}_n$ ($i = 1-x, 1-y, -z$; $ii = -x, 1-y, -z$). (b) Final 1D polymeric chains propagated along the c crystallographic axis. (c) Content of unit cell.

of X-ray diffraction studies show that the compound crystallizes in a triclinic lattice with space group P , having cell parameters $a = 5.3994(2)$ Å, $b = 8.8389(4)$ Å, $c = 10.5007(5)$ Å, $\alpha = 101.207(2)^\circ$, $\beta = 95.930(2)^\circ$, and $\gamma = 93.338(2)^\circ$. The asymmetric unit is formed from one cadmium(II), one PDA-Cl ligand and two water molecules coordinated in different modes. Cd(II) ions are seven-coordinate and the coordination polyhedron could be described as a distorted pentagonal bipyramid. The equatorial plane is formed from three oxygens (O1, O1ⁱ and O3; $i = 1-x, 1-y, -z$), one nitrogen (N1) of two DPA-Cl molecules and a coordinated water (O5). The axial positions are occupied by two oxygens (O6 and O5ⁱⁱ, $ii = -x, 1-y, -z$) of two different water molecules as depicted in Figure 4a. Both carboxylic groups of H₂PDA-Cl acid are deprotonated and coordinated to cadmium in different coordination modes. Carboxylate with C4 is monodentate mode and carboxylate (C1) makes a bridge between two cadmium(II) ions via O1. The distances between cadmium(II) ions and carboxylate oxygens are 2.3469(18)–2.4286(18) Å and are typical for similar cadmium carboxylate compounds [28, 29, 30, 31]. Pyridine nitrogen of PDA-Cl ligand is coordinated to cadmium with shorter bond length 2.299(2) Å, indicating stronger interaction with Cd(II). As mentioned above, there are two water molecules coordinated in different coordination fashion in the crystal structure of **2**. Water molecule (O6) is terminally coordinated to Cd(II) with bond length 2.2944(19) Å and the other water molecule (O5) generates a bridge between two cadmium ions; the Cd-O5 bond is therefore longer (2.3145(19) Å, Supplementary Information Table S5). The bond angles around cadmium(II) indicate distortion from ideal pentagonal-bipyramidal geometry, which is reflected especially in the axial angle O6-Cd-O5ⁱⁱ of 155.588(61) $^\circ$ and in the equatorial bite angles O3-Cd-N1 (69.560(67) $^\circ$), N1-Cd-O1 (68.306(66) $^\circ$), O1-Cd-O1ⁱ (73.626(68) $^\circ$), O1ⁱ-Cd-O5 (74.614(62) $^\circ$) or O5-Cd-O3 (76.248(66) $^\circ$).

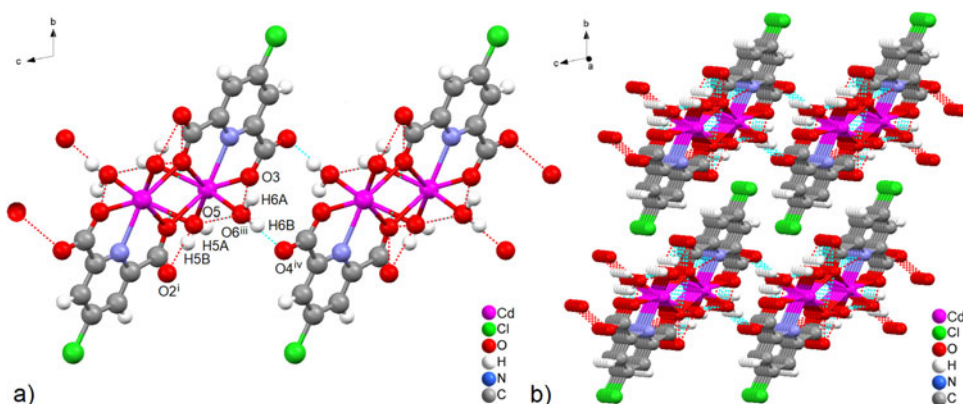


Figure 5. (a) Intramolecular and intermolecular hydrogen bonds in $\{[\text{Cd}(\mu_2\text{-H}_2\text{O})(\text{H}_2\text{O})(\text{PDA-Cl})]\}_n$ ($i = 1-x, 1-y, -z$; $\text{iii} = x-1, y, z$; $\text{iv} = -x, -y, -z$). (b) View of the final supramolecular 2D polymeric sheets propagated along ac crystallographic plane.

Because of one bridging carboxylate O and two bridging water molecules, the adjacent cadmium(II) ions are joined to the formation of 1D polymeric chains propagating along the a crystallographic axis (Figure 4b). Cadmium ions are arranged in zig-zag chains with $\text{Cd}\cdots\text{Cd}$ separation of 3.7164(3) Å for Cd-Cd^{ii} and 3.8235(3) Å for Cd-Cd^{i} .

Due to the presence of water molecules in the crystal structure of **2**, there is a rich network of hydrogen bonds (Figure 5). Intramolecular hydrogen bonds are formed between bridging water (O5) acting as donor, while the acceptor is O6 of the terminal water molecule having both the $\text{O5-H5A}\cdots\text{O6}^{\text{iii}}$ ($\text{iii} = x-1, y, z$) distance 2.819(3) Å and the carboxylate oxygen O2 with $\text{O5-H5B}\cdots\text{O2}^{\text{i}}$ distance 2.578(3) Å. The water O6 creates an intermolecular hydrogen bond as donor with carboxylate O4 from an adjacent polymeric chain with $\text{O6-H6B}\cdots\text{O4}^{\text{iv}}$ ($\text{iv} = -x, -y, -z$) distance of 2.608(3) Å. The polymeric chains are stabilized in the solid state by hydrogen bonds with formation of supramolecular 2D polymeric sheets propagating along the ac crystallographic plane (Figure 5b). Corresponding hydrogen bond lengths and angles are summarized in Supplementary Information Table S6.

Similar coordination of ligands to cadmium(II) ions was observed in $\{[\text{Cd}_2(\text{DPA-OH})_2(\text{H}_2\text{O})_2]\cdot 4\text{H}_2\text{O}\}_n$ [32] and $\{[\text{Cd}_2(\text{DPA-OH})_2(\text{H}_2\text{O})_2]\cdot 0.5\text{MeOH}\cdot 3\text{H}_2\text{O}\}_n$ [33] (DPA-OH = 4-hydroxypyridine-2,6-dicarboxylate, chelidamate). The compounds are also seven-coordinate binuclear polymeric complexes with distorted pentagonal bipyramidal geometry around Cd(II). In their binuclear monomeric units, cadmiums are joined by the O atoms of two bridging tridentate DPA-OH ligands and the polymer propagates via two bridging water molecules that link each Cd(II) of one monomer to the neighbor. Their Cd–O and Cd–N distances are in the same range as **2**. The difference between **2** and Cd-chelidamate complexes is in the number and type of crystallization solvent molecules, which separate 1D chains from each other and are able to form different types of hydrogen bonds.

3.2. Infrared spectroscopy

Comparing IR spectra of H_2PDA and $\text{H}_2\text{PDA-Cl}$ (Supplementary Information Figure S1), the absorptions slightly change their positions, attributed to the chlorine in the *ortho* position.

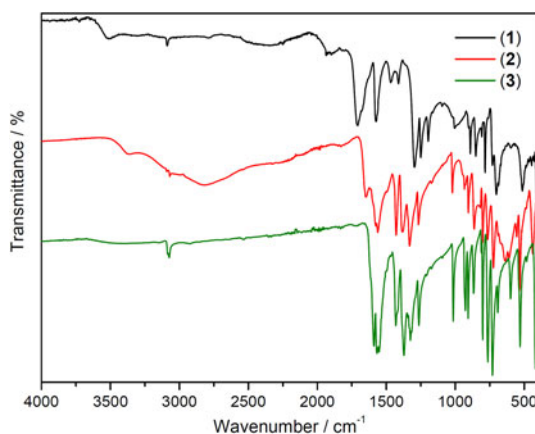


Figure 6. Infrared spectra of prepared compounds.

Table 2. The IR spectral data assignments for H₂DPA, H₂DPA-Cl and 1-3 (band positions are in cm⁻¹).

| Assignments | Wavenumbers (cm ⁻¹) and intensities | | | | |
|--|---|----------------------|------------------|------------------|------------------|
| | H ₂ PDA | H ₂ PDACl | 1 | 2 | 3 |
| $\nu(\text{OH})$ | | 3479(w) | 3490(w) | 3330(vw) | |
| $\nu(\text{CH})$ | 3065(w) | 3092(w) | 3089(w) | 3060(w) | 3074(w) |
| $\nu(\text{C}=\text{O})$ | 1692(s) | 1726(s) | 1707(m) | | |
| $\nu_{\text{as}}(\text{COO}^-)$ | | | 1660(w) | 1645(w) | 1590(s) |
| $\nu(\text{C}=\text{C})$ | 1573(m) | 1575(m) | 1573(m) | 1562(m) | 1569(s) |
| $\nu(\text{C}=\text{N})$ | 1454(m) | 1477(w) | 1468(m) | 1428(m) | 1430(s) |
| $\nu_{\text{s}}(\text{COO}^-)$ | 1411(m) | 1439(w) | 1412(m) | 1385(m) | 1371(s) |
| $\nu(\text{C}-\text{O})+\delta(\text{OH})$ | 1295(m), 1263(m) | 1311(s), 1211(m) | 1295(m), 1250(m) | 1330(m), 1266(m) | 1311(m), 1263(m) |
| $\delta(\text{CCH})$ | 1161(m), 1079(m) | 1170(s), 1050(w) | 1003(w) | 1021(w) | 1014(m) |
| $\gamma(\text{CCH})$ | 783(s), 748(s) | 783(m), 729(m) | 783(m) | 765(w), 723(m) | 764(s), 730(s) |
| $\delta(\text{COO}^-)$ | 692(s), 646(s) | 677(s) | 702(m) | 640(m) | 600(m) |
| $\Delta(\nu_{\text{as}} - \nu_{\text{s}})_{\text{exp}}$ | | | 248 | 260 | 219 |
| $\Delta(\nu_{\text{as}} - \nu_{\text{s}})_{\text{calc}}$ | | | 246 | 234 | |

s, strong; m, medium; w, weak.

Comparing to IR data of complexes, the observed shifts and splitting of corresponding bands reveal ligand coordination to Ag(I), Cd(II) even the Pb(II). The water molecule and hydrogen bonds in the structure are associated with stretching vibrational mode $\nu(\text{O-H})$ at 3479 (for H₂PDA-Cl), 3490 (for **1**) and 3330 cm⁻¹ (for **2**), similar to the terbium(III) complexes with 4-substituted dipicolinic acid analogues [13] and silver dipicolinate complex [26, 27]. Contrary, IR spectra indicate anhydrous complex **3**, because of absence of $\nu(\text{O-H})$ (Figure 6). Furthermore, significant band at 1707 cm⁻¹ confirms the carbonyl stretching vibration in **1** that is in accordance with structural data. The characteristic free carboxylic acid vibrations, $\nu(\text{C}=\text{O})$ and $\nu(\text{C}-\text{O})$, are converted to asymmetric, $\nu_{\text{as}}(\text{COO})$, and symmetric, $\nu_{\text{s}}(\text{COO})$ stretching vibrations of carboxylate as expected after its coordination to central atom in **1**, **2**, and **3** that also confirm its bond distances and angles change in free ligand and in complexes (Section 3.1). The wavenumber difference, $\Delta(\nu_{\text{as}} - \nu_{\text{s}})$, is consistent with monodentate coordination of the carboxylate to Ag(I), Cd(II), and Pb(II) (Table 2), in agreement with structural results (carboxylate monodentate coordination mode). The same monodentate coordination mode was assigned to dipicolinate for Cd(II) and Pb(II)

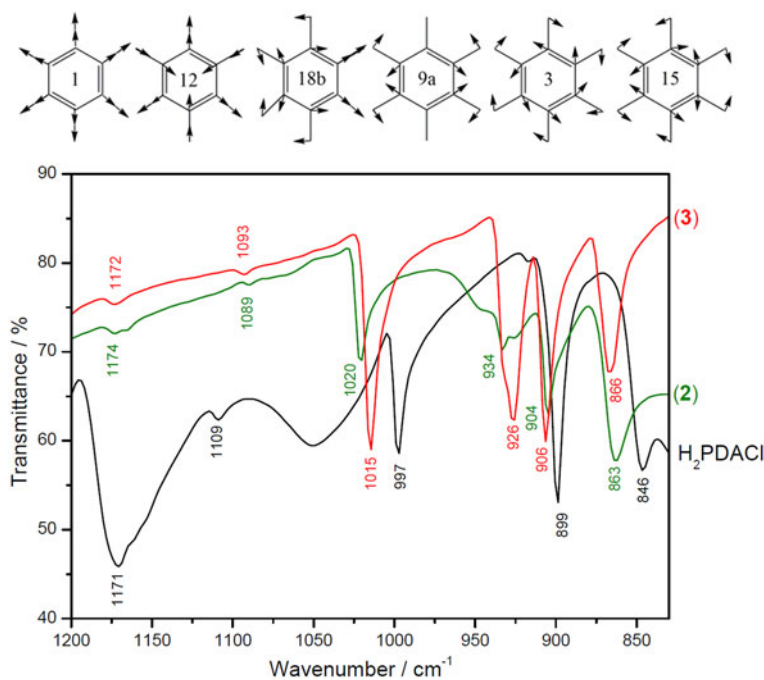


Figure 7. Scheme of *in-plane* bending vibrations with Wilson's notation and comparison of cadmium(II), lead(II) compound and free H₂PDA-Cl ligand in wavenumber region 1200–800 cm⁻¹.

complexes, $\Delta(\nu_{as} - \nu_s) = 212$ and 220 cm⁻¹, respectively [28, 34]. However, $\nu_{as}(\text{COO})$ at lower wavenumber ($1587, 1700$ cm⁻¹ [28, 34]) than in **2** (1645 cm⁻¹) and in **3** (1590 cm⁻¹). Similar differences were observed for symmetric stretching vibrations in the case of Cd(II) complexes (1375 cm⁻¹ for a Cd(II) complex [28], 1385 cm⁻¹ for **2**). However, symmetric stretch comparison (in the case of Pb(II) complexes), 1480 cm⁻¹ for Pb(II) complex [34] and 1371 cm⁻¹ for **3**, respectively. This points to the fact that carboxylates are involved in different systems of hydrogen bonds.

Both deformation vibrations were observed in all cases (ligands and **1**, **2**, and **3**), the *in-plane* bending modes $\delta(\text{CCH})$ from 1180 to 800 cm⁻¹ and *out-of-plane* bending modes $\gamma(\text{CCH})$ from 790 to 600 cm⁻¹ (Table 2).

Additionally, to confirm PDA-Cl coordination to Pb(II) we correlated pyridine ring *in-plane* bending vibrations of free ligand and **2** (crystalline products with deprotonated ligand in the structure) and **3** (precipitate product). The pyridine ring vibrations are 1200 to 850 cm⁻¹ [35]. The typical ring vibrations in accordance with Wilson's notation [36] at $964, 995(1), 1007, 1045(12), 1044, 1085, (18b), 1083, 1093(9b), 1250, 1254(15), 1292, 1292(3)$ cm⁻¹ were noted for PIC and AgPIC [37]. Significant changes were observed in the case of PDA-Cl ligand and its Cd(II) and Pb(II) complexes comparing mentioned bands range. The free ligand pyridine ring vibrations were noted at $846(1), 899(12), 997(18b), 1109(9b), 1171(3, 15)$. Spectra indicate **3** and **15** vibrations overlap. *In-plane* bending vibrations **1**, **12**, **18b** and **15** (and **3**) change their positions to higher wavenumbers and **9b** to lower values in **2** and **3** (Figure 7). Observed wavenumber shifts confirm PDA-Cl ligand coordination to Pb(II) in **3**.

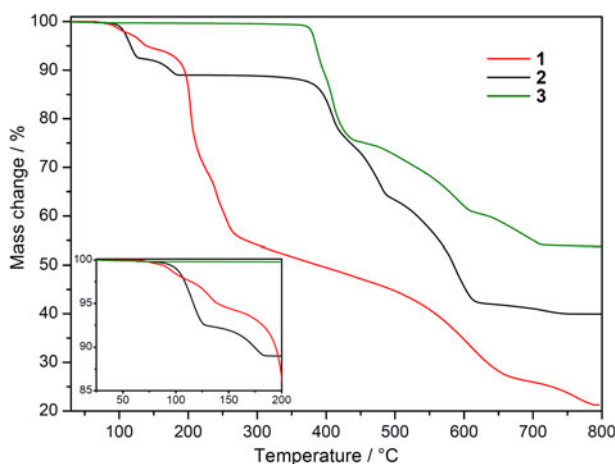


Figure 8. Thermoanalytical curves of prepared complexes (a) $[\text{Ag}(\text{H}_2\text{PDA-Cl})(\text{HPDA-Cl})]\cdot 2\text{H}_2\text{O}$, (b) $\{[\text{Cd}(\mu_2\text{-H}_2\text{O})(\text{H}_2\text{O})(\text{PDA-Cl})]\}_n$ and (c) $[\text{Pb}(\text{PDA-Cl})]$ measured in air atmosphere. Inset shows a detailed view on the dehydration process of compounds in temperature range 30–200 °C.

3.3. Thermal analysis

To estimate the thermal stability of our compounds, thermogravimetric analysis was carried out under air (TG curves shown in Figure 8). $[\text{Ag}(\text{H}_2\text{PDA-Cl})(\text{HPDA-Cl})]\cdot 2\text{H}_2\text{O}$ is thermally stable after heating at 70 °C (inset of Figure 8). Above this temperature, 70–155 °C, dehydration of **1** takes place in two decomposition steps. In mentioned temperature range total mass loss of 6.41% was observed and corresponds to release of two crystallization water molecules (Anal Calcd mass loss 6.60%). Observed decomposition step could be divided into two separate processes in which step-by-step dehydration of water molecules takes place, from 70–110 °C (mass loss observed 3.18%, calculated 3.30%) and 110–155 °C (mass loss observed 3.23%, calculated 3.30%). At higher temperature, decomposition of anhydrous complex occurs. From 155 to 270 °C mass loss of 38.36% was observed (Anal calcd mass loss 36.91%) followed with two steps on TG curve and this process was assigned to loss of $\text{H}_2\text{PDA-Cl}$ molecule. This molecule is fully protonated and bonded with less energy compared to deprotonated form of the ligand, which forms stronger interactions. Therefore, this molecule is evolved before HPDA-Cl^- ligand. Based on literature data it is known that $\text{H}_2\text{PDA-Cl}$ melts at 210 °C and evaporates [38]. Similar thermal behavior was also observed in $\{\text{Ag}(\text{INA})_3(\text{HINA})\}_n$ (INA – isonicotinate), where protonated and deprotonated forms of isonicotinate are present. In the first stage of thermal decomposition HINA was evolved and then release of INA^- ligands occurred [39]. The thermal decomposition of **1** ends at 780 °C and final decomposition product was elemental silver (obs. residual mass 21.28%, Anal Calcd residual mass 19.76%).

As can be seen from the TG curve for $\{[\text{Cd}(\mu_2\text{-H}_2\text{O})(\text{H}_2\text{O})(\text{PDA-Cl})]\}_n$ (Figure 8), **2** is stable in air to 85 °C. When heating above this temperature, release of coordinated water takes place. Dehydration occurs in two decomposition steps from 85 to 185 °C, first step at 85–125 °C with mass loss of 7.42% and the second step at 125–185 °C with mass loss of 3.57%. Observed mass changes were attributed to the gradual release of 1.5 moles (Anal. calcd mass loss 7.76%) and 0.5 mole (Anal. calcd mass loss 2.59%) of water molecules (inset

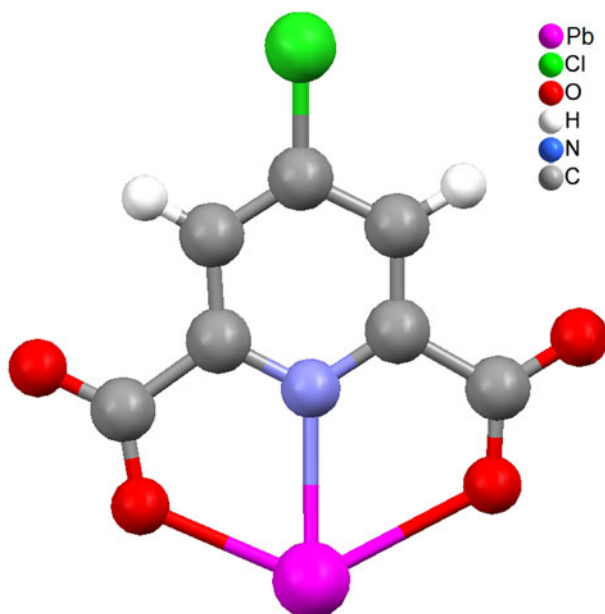


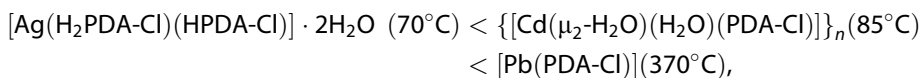
Figure 9. Proposed molecular diagram of **3** derived from spectral and thermal studies.

of **Figure 8**). The total observed mass loss of the dehydration process is 10.35% (Anal. Calcd mass loss 10.99%) and corresponds to the release of two water molecules, in agreement with the crystal structure and the chemical composition of **2**. The dehydrated form of **2** is thermally stable from 185 to 380 °C as is seen from the plateau on the TG curve (**Figure 8**). The decomposition of $\{[\text{Cd}(\text{PDA}-\text{Cl})]\}_n$ takes place in four overlapping decomposition steps. In the first stage loss of chlorine from $\text{PDA}-\text{Cl}^{2-}$ occurs, which was reflected by the mass change 10.60% on TG from 380 to 420 °C (Anal. Calcd mass loss 10.19%). In further decomposition steps thermal decomposition of residual organic moiety (probably dipicolinate, PDA^{2-}) occurs and decomposition ends at 750 °C. Final product of thermal decomposition was CdO (obs. residual mass 39.94%, Anal. calcd residual mass 38.67%). Similar polymeric complex containing the same building blocks (water, Cd(II) ions) was prepared with dipicolinic acid with composition $\{[\text{Cd}(\text{H}_2\text{O})_{1.5}(\text{PDA})]\}_n$. After dehydration (150–220 °C) this complex is stable to 330 °C [28]. When we compare thermal stability of anhydrous forms for **2** and Cd(II)-dipicolinate complex, it is obvious that $\{[\text{Cd}(\text{PDA}-\text{Cl})]\}_n$ framework is more stable. This observation could be explained by positive mesomeric effect of chloro substituent in molecular structure of 4-chloropyridine-2,6-dicarboxylate ligand. It is apparent that an electron-releasing group enhances the binding strength between the carboxylate group and the central atom, which is reflected in higher thermal stability.

As predicted by IR spectroscopy, $[\text{Pb}(\text{PDA}-\text{Cl})]$ was prepared in anhydrous state (see **Section 3.2**) and TG analysis also confirmed this presumption. As can be seen from the TG curve (**Figure 8**), **3** is thermally stable from 30 to 370 °C without significant mass change. The decomposition of organic part occurs in four stages as in **2**. In the first stage chlorine is evolved from 370 to 400 °C with observed mass loss 8.29%, which is in agreement with calculated value 8.72%. The decomposition of dipicolinic acid takes

place in the next three overlapping stages from 400 to 710 °C (obs. mass loss 37.36%, Anal. calcd mass loss 36.41%). The final product of thermal decomposition of **3** was PbO (obs. residual mass 55.45%, Anal. calcd residual mass 54.87%).

Based on the obtained results, the thermal stability of the prepared compounds can be arranged in the following order:



and for anhydrous forms in following order:



The conclusion of thermal behavior for anhydrous compounds can be summarized as follows: lower thermal stability of the silver(I) complex could be explained due to the presence of the protonated ($\text{H}_2\text{PDA-Cl}$), which forms weak interactions with the central atom and therefore is released at a lower temperature. In the case of the cadmium(II) and lead(II) complexes, their thermal stability is comparable, because of deprotonated ligand in both compounds (PDA-Cl^{2-}), which could form strong ion–ion interaction with central atoms. The increased thermal stability of the cadmium complex can be explained by the polymeric nature of the complex.

4. Conclusion

A new series of 4-chloro-dipicolinate metal complexes has been prepared and characterized. The single crystal structure reveal the asymmetric unit formed from one silver(I), one ligand molecule and one crystallization water molecule in the case of **1**. Each PDA-Cl ligand acts as a tridentate ligand of Ag(I), through the pyridine N and two monodentate carboxyl O atoms. In the case of **2** the asymmetric unit is formed from one cadmium(II) ion, one PDA-Cl ligand and two water molecules coordinated in different modes. Cd(II) ions are seven-coordinate in a distorted pentagonal bipyramid.

The spectral, thermal and elemental analysis comparison confirms the $[\text{Pb}(\text{PDA-Cl})]$ empirical formula for **3**. The wavenumber differences, $\Delta(\nu_{as} - \nu_s)$, are consistent with monodentate coordination of the carboxylate to Ag(I), Cd(II), and Pb(II), in agreement with structural results (carboxylate monodentate coordination mode). Moreover, PDA-Cl, **2** and **3** *in-plane* bending vibrations (by Wilson's notation) confirm PDA-Cl ligand coordination to Pb(II).

The thermal stability of the anhydrous compounds can be arranged in the following order: $[\text{Ag}(\text{H}_2\text{PDA-Cl})(\text{HPDA-Cl})]$ (155 °C) < $[\text{Pb}(\text{PDA-Cl})]$ (370 °C) < $\{[\text{Cd}(\text{PDA-Cl})]\}_n$ (380 °C) and can be explained by the presence of the protonated ligand molecule ($\text{H}_2\text{PDA-Cl}$) in the silver(I) complex and deprotonated ligand molecule (PDA-Cl) in cadmium(II) and lead(II) complexes.

From infrared spectroscopy and thermal analysis we proposed the molecular diagram of **3** (Figure 9).

Disclosure statement

No potential conflict of interest was reported by the authors.

Funding

This work was supported by the Ministry of the Education, Science, Research and Sport of the Slovak Republic [grant number KEGA 008UPJS-4/2018]. Authors Z.V. and M.A. thank for the financial support of the TRIANGEL team in the frame of the scheme "Top Research Teams in Slovakia". R.Gy. is grateful to OP VVV "Excellent Research Teams" (Project No. CZ.02.1.01/0.0/0.0/15_003/0000417 – CUCAM).

References

- [1] Z. Hubicki, D. Kołodzyńska, *Ion Exchange Technologies*, p. 193, InTech, Rijeka (2012).
- [2] I.S.S. Pinto, I.F.F. Neto, H.M.V.M. Soares, *Environ. Sci. Pollut. Res.*, **21**, 11893 (2014).
- [3] J.G. Martins, I.F.F. Neto, I.S.S. Pinto, E.V. Soares, M.T. Barros, H.M.V.M. Soares, *J. Environ. Sci. Health., Part A*, **49**, 344 (2014).
- [4] Z. Xu, L.K. Thompson, D.O. Miller, *Polyhedron*, **21**, 1715 (2002).
- [5] J.J. Smee, J.A. Epps, K. Ooms, S.E. Bolte, T. Polenova, B. Baruah, L. Yang, W. Ding, M. Li, G.R. Willisky, A. La Cour, O.P. Anderson, D.C. Crans, *J. Inorg. Biochem.*, **103**, 575 (2009).
- [6] S.J. Cline, S. Kallesoe, E. Pedersen, D.J. Hodgson, *Inorg. Chem.*, **18**, 796 (1979).
- [7] T.L. Kelly, V.A. Milway, H. Grove, V. Niel, T.S.M. Abedin, L.K. Thompson, L. Zhao, R.G. Harvey, D.O. Miller, M. Leech, A.E. Goeta, J.A.K. Howard, *Polyhedron*, **24**, 807 (2005).
- [8] S. Abdolmaleki, M. Ghadermazi, A. Fattahi, S. Sheshmani, *Inorg. Chim. Acta*, **443**, 284 (2016).
- [9] C.C. Ou, R.G. Wollmann, D.N. Hendrickson, J.A. Potenza, H.J. Schugar, *J. Am. Chem. Soc.*, **100**, 4717 (1978).
- [10] S. Abdolmaleki, M. Ghadermazi, A. Fattahi, S. Shokraii, M. Alimoradi, B. Shahbazi, A.R. Judy Azar, *J. Coord. Chem.*, **70**, 1406 (2017).
- [11] P.M. Cantos, S.J.A. Pope, C.L. Cahill, *CrystEngComm*, **15**, 9039 (2013).
- [12] M.J. Shaw, P. Jones, P.N. Nesterenko, *J. Chromatogr. A*, **953**, 141 (2002).
- [13] J. Lamture, J.B. Lamture, Z. Zhou, Z.H. Zhou, S. Kumar, T.G. Wensel, *Inorg. Chem.*, **34**, 864 (1995).
- [14] M.R. George, C.A. Golden, M.C. Grossel, R.J. Curry, *Inorg. Chem.*, **45**, 1739 (2006).
- [15] G.M. Sheldrick, *Acta Crystallogr. C Struct. Chem.*, **C71**, 3 (2015).
- [16] K. Brandenburg, *Diamond Version 3.2k, 1997–2004*, Crystal Impact GbR, Bonn, Germany (2012).
- [17] C.F. Macrae, I.J. Bruno, J.A. Chisholm, P.R. Edgington, P. McCabe, E. Pidcock, L. Rodriguez-Monge, R. Taylor, J. van de Streek, P.A. Wood, *J. Appl. Crystallogr.*, **41**, 466 (2008).
- [18] Origin[®] v 6.1052 (B232) by OriginLab, Northampton, MA.
- [19] M. Nieger, F. Vögtle, W.M. Müller, CSD Communications. Deposition Number(s): 1819428 (2018). DOI: [10.5517/ccdc.csd.cc1z287k](https://doi.org/10.5517/ccdc.csd.cc1z287k)
- [20] M.C. Grossel, A.N. Dwyer, M.B. Hursthouse, J.B. Orton, *CrystEngComm*, **9**, 207 (2007).
- [21] J. Zheng, D. Zhou, T.H. Shi, Q.Q. Guan, Y. Xu, *J. Coord. Chem.*, **67**, 533 (2014).
- [22] Y. Song, R. Fan, X. Du, K. Xing, P. Wang, Y. Dong, Y. Yang, *CrystEngComm*, **18**, 6411 (2016).
- [23] P. Thuery, J. Harrowfield, *Cryst. Growth Des.*, **16**, 7083 (2016).
- [24] R.S. Zhou, J.F. Song, *Acta Crystallogr. Sect. E Struct. Rep. Online*, **65**, m1523 (2009).
- [25] Y.G. Sun, M.Y. Guo, G. Xiong, F. Ding, L. Wang, B. Jiang, M.C. Zhu, E.J. Gao, F. Verpoort, *J. Coord. Chem.*, **63**, 4188 (2010).
- [26] M.G.B. Drew, R.W. Matthews, R.A. Walton, *J. Chem. Soc. A*, 1405 (1970).
- [27] Y. Wang, M. Odoko, N. Okabe, *Acta Crystallogr. E Struct. Rep. Online*, **60**, m1178 (2004).
- [28] B.M. Kukovec, G.A. Venter, C. L. Oliver, *Cryst. Growth Des.*, **12**, 456 (2012).
- [29] B.M. Kukovec, C. L. Oliver, *Polyhedron*, **34**, 46 (2012).
- [30] A. Moghimi, S. Sheshmani, A. Shokrollahi, H. Aghabozorg, M. Shamsipur, G. Kickelbick, M. Car Aragoni, V. Lippolis, *Z. Anorg. Allg. Chem.*, **630**, 617 (2004).

- [31] E.V. Brusau, J.C. Pedregosa, G.E. Narda, G. Pozzi, G. Echeverria, G. Punte, *J. Coord. Chem.*, **54**, 469 (2001).
- [32] H. Aghabozorg, N. Ilaie, M. Heidari, F. Manteghi, H. Pasdar, *Acta Crystallogr. E Struct. Rep. Online*, **64**, m1351 (2008).
- [33] J.P. Zou, X.M. Liu, L.S. Yan, A.M. Deng, Q.J. Xing, M.H. Chen, *J. Coord. Chem.*, **63**, 56 (2010).
- [34] H. Eshtiagh-Hosseini, H. Aghabozorg, M. Mirzaei, M.M. Amini, Y.-G. Chen, A. Shokrollahi, R. Aghaei, *J. Mol. Struct.*, **973**, 180 (2010).
- [35] K. Nakamoto, *Infrared and Raman Spectroscopy of Inorganic and Coordination Compounds*, (Part B), 6th Edn, Wiley, New York (1997).
- [36] E. Bright Wilson. *Phys. Rev.*, **45**, 706 (1934).
- [37] Z. Vargová, M. Al máši, D. Hudcová, D. Titková, I. Rostášová, V. Zelenák, K. Györyová. *J. Coord. Chem.*, **67**, 1002 (2014).
- [38] A.R. de la Faverie, F. Hamon, C.D. Primo, E. Largy, E. Dausse, L. Delaurière, C. Landras-Guetta, J.J. Toulmé, M.P. Teulade-Fichou, J.L. Mergny, *Biochimie*, **93**, 1357 (2011).
- [39] M. Al máši, Z. Vargová, D. Sabolová, J. Kudláčová, D. Hudcová, J. Kuchár, L. Očenášová, K. Györyová, *J. Coord. Chem.*, **68**, 4423 (2015).